J|A|C|S ARTICLES

Published on Web 08/16/2010

Quantized Folding of Plasmid DNA Condensed with Block Catiomer into Characteristic Rod Structures Promoting Transgene Efficacy

Kensuke Osada,[†,§] Hiroki Oshima,[†] Daigo Kobayashi,[†] Motoyoshi Doi,[†] Manabu Enoki,[†] Yuichi Yamasaki,[†,§] and Kazunori Kataoka*[,†,‡,§]

Department of Materials Engineering, Graduate School of Engineering, Division of Clinical Biotechnology, Center for Disease Biology and Integrative Medicine, Graduate School of Medicine, and Center for NanoBio Integration, The University of Tokyo, 7-3-1 Hongo, Bunkyo-ku, Tokyo 113-8656, Japan

Received April 1, 2010; E-mail: kataoka@bmw.t.u-tokyo.ac.jp

Abstract: Highly regulated folding of plasmid DNA (pDNA) through polyion complexation with the synthetic block catiomer, poly(ethylene glycol)-*block*-poly(L-lysine) (PEG-PLys), was found to occur in such a way that rod structures are formed with a quantized length of $1/2(n+1)$ of the original pDNA length folding by n times. The folding process of pDNA was elucidated with regard to rigidity of the double-stranded DNA structure and topological restriction of the supercoiled closed-circular form, and a mechanism based on Euler's buckling theory was proposed. Folded pDNA exhibited higher gene expression efficiency compared to naked pDNA in a cell-free transcription/translation assay system, indicating that the packaging of pDNA into a polyion complex core surrounded by a PEG palisade is a promising strategy for constructing nonviral gene carrier systems. Extension of this finding may provide a reasonable model to further understand the packaging mechanism of supercoiled DNA structures in nature.

Introduction

DNA remarkably changes its excluded volume upon polyion complexation with cationic compounds, and this phenomenon is exploited in natural genome containers such as the cell nucleus, nucleoids, and viral capsids. The large volume transition from a coil to a globular state,[1,2] known as DNA condensation,[3,4] is at the core of biological processes such as a chromatin formation. Plasmid DNA (pDNA) comprises a characteristic supercoiled closed-circular topology[5−7] and has received much attention in biology, chemistry, and topological mathematics because it is considered to be an intermediate structure in DNA evolution, found in primitive genomes such as viruses, prokaryotes, and mitochondria. Condensation of pDNA is also highlighted due to its practical importance for medical applications such as gene therapy.[8−14] The condensation process is rather complex, as stresses such as bending and torsion must be relaxed within the constraints of the unique topology of supercoiling and the rigidity of double-stranded DNA.[15] It is known that condensation of pDNA results in folded-fiber rod structures (rods), donut-like structures (toroids), and collapsed sphere structures;[16−18] however, the condensation mechanism is not yet fully understood. This lack of clarity is mainly due to the difficulty involved with tracking the condensation process of a single pDNA molecule upon complexation with cationic compounds, as intercomplex aggregation results in the formation of phase-separated precipitates. Furthermore, observation tools such as fluorescence microscopy[19,20] are not applicable, as pDNA is not large enough to obtain sufficient resolution. To address these issues, we used here block catiomers comprising a neutral hydrophilic poly(ethylene glycol) (PEG) segment and a cationic poly(L-lysine) (PLys) segment as pDNA condensing agents, along with transmission electron microscopy (TEM) and atomic force microscopy (AFM) as tools for detailed structural observation. Upon mixing with block catiomers,

[†] Graduate School of Engineering.
[‡] Graduate School of Medicine.
[§] Center for NanoBio Integration.

(1) Stockmayer, W. H. *Makromol. Chem.* **1960**, *35*, 54–74.
(2) Melnikov, S. M.; Sergeyev, V. G.; Yoshikawa, K. *J. Am. Chem. Soc.* **1995**, *117*, 2401–2408.
(3) Laemmli, U. K. *Proc. Natl. Acad. Sci. U.S.A.* **1975**, *72*, 4288–4292.
(4) Bloomfield, V. A. *Curr. Opin. Struct. Biol.* **1996**, *6*, 334–341.
(5) Palecek, E. *Crit. Rev. Biochem. Mol. Biol.* **1991**, *26*, 151–226.
(6) Podtelezhnikov, A. A.; Cozzarelli, N. R.; Vologodskii, A. V. *Proc. Natl. Acad. Sci. U.S.A.* **1999**, *96*, 12974–12979.
(7) Bronich, T. K.; Nguyen, H. K.; Eisenberg, A.; Kabanov, A. V. *J. Am. Chem. Soc.* **2000**, *122*, 8339.
(8) Kabanov, A. V.; Kabanov, V. A. *Bioconjugate Chem.* **1995**, *6*, 7.
(9) Kataoka, K.; Harada, A.; Nagasaki, Y. *Adv. Drug Delivery Rev.* **2001**, *47*, 113–131.
(10) Pack, D. W.; Hoffman, A. S.; Pun, S.; Stayton, P. S. *Nat. Rev. Drug Discovery* **2005**, *4*, 581–593.
(11) Osada, K.; Kataoka, K. *Adv. Polym. Sci.* **2006**, *202*, 113–153.
(12) Mastrobattista, E.; van der Aa, M. A. E. M.; Hennink, W. E.; Crommelin, D. J. A. *Nat. Rev. Drug Discovery* **2006**, *5*, 115–121.
(13) Wagner, E.; Kloeckner, J. *Adv. Polym. Sci.* **2006**, *192*, 135.
(14) Haag, R.; Kratz, F. *Angew. Chem., Int. Ed.* **2006**, *45*, 1198.
(15) Eisenberg, H. *Acc. Chem. Res.* **1987**, *20*, 276–282.
(16) Eickbush, T. H.; Moudrianakis, E. N. *Cell* **1978**, *13*, 295–306.
(17) Bloomfield, V. A. *Biopolymers* **1997**, *44*, 269–282.
(18) Golan, R.; Pietrasanta, L. I.; Hsieh, W.; Hansma, H. G. *Biochemistry* **1999**, *38*, 14069–14076.
(19) Minagawa, K.; Matsuzawa, Y.; Yoshikawa, K.; Matsumoto, M.; Doi, M. *FEBS Lett.* **1991**, *295*, 67–69.
(20) Yamasaki, Y.; Katayose, S.; Kataoka, K.; Yoshikawa, K. *Macromolecules* **2003**, *36*, 6276.

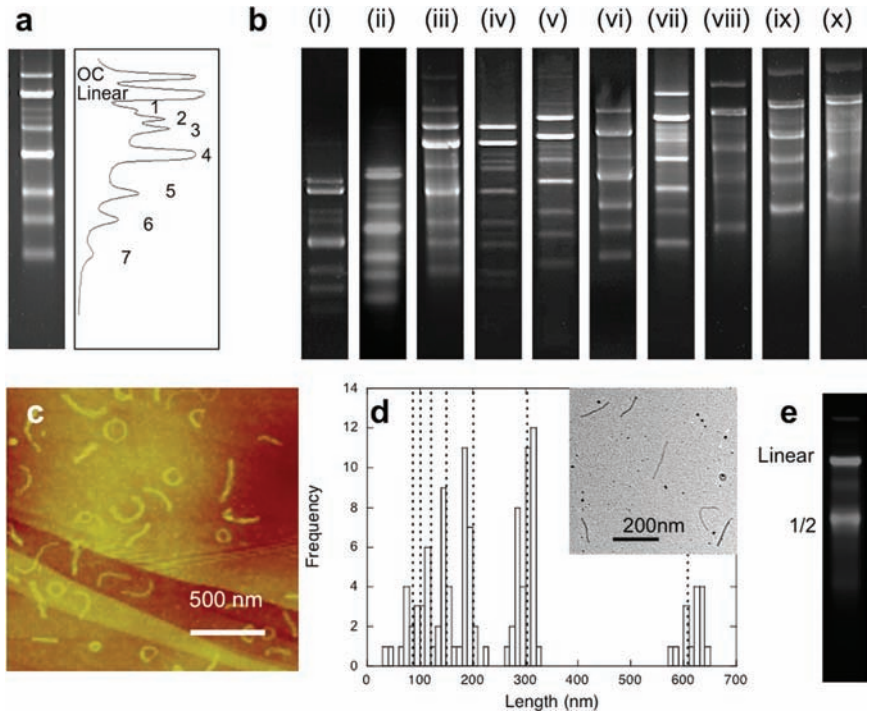

Figure 1. Folding of pDNA induced by complexation with PEG-PLys block catiomer at an N/P ratio of 1. (a) S1 nuclease activity toward complexed pBR322 visualized by gel electrophoresis and corresponding intensity profiles obtained by densitometry. Bands corresponding to relaxed open-circular ("OC") DNA, linearized ("linear") DNA, and digested fragments (1−7) are indicated in the profiles. (b) S1 nuclease activity toward a series of the complexed pDNAs: (i) pKF18 (2204 bp), (ii) pUC19 (2686 bp), (iii) luciferase T7 control DNA (4315 bp), (iv) pBR322 (4361 bp), (v) pGL3-Luc (5256 bp), (vi) ϕX174 (5386 bp), (vii) ColE1 (6646 bp), (viii) pAUR224 (7638 bp), (ix) pPTR2 (10032 bp), and (x) pAUR316 (11613 bp). (c) AFM image of complexed pDNA (pBR322) recorded in height mode. (d) Distribution of long axis lengths of the complexed pBR322 rod structures measured from TEM images. A total of 250 individual rods were subjected to the measurement. Inset: representative TEM image (additional TEM images are provided in the Supporting Information, Figure S3). Dotted lines in the figure indicate theoretically calculated lengths based on the quantized folding model. (e) S1 nuclease activity toward pBR322 complexed with PEG-PLys block catiomer prepared at N/P = 0.75.

pDNA is condensed into a polyion complex core surrounded by a PEG shell, and condensation of a single pDNA eventually occurs without intercomplex aggregation.[21−24] This scheme for polyion complex formation provides a unique system that allows for detailed observation of DNA condensation processes, even upon complete charge-neutralization, which is extremely difficult to observe in non-PEGylated systems due to aggregation. Furthermore, the activity of S1 nuclease, which is known to cleave single-stranded DNA, toward pDNA condensed by PEG-PLys block catiomer was observed, and pDNA was cleaved into distinctly ordered fragments corresponding to 2/12, 3/12, 4/12, 6/12, 8/12, 9/12, and 10/12 of the original pDNA length.[25] This S1 nuclease activity suggests that double-strand dissociation of pDNA into a single strand is induced at well-regulated sites. In this regard, S1 nuclease activity is an attractive tool for studying the pDNA condensation mechanism related to double-stranded DNA rigidity, characteristic topological constraints, and morphological variation.

Through these experiments, we reveal here, for the first time, the regulated folding mechanism of pDNA condensation into quantized-length rods, being $1/2(n + 1)$ of the pDNA contour length (n indicates the folding number), through dissociation of the double-stranded structure at every folding site upon polyion complexation with block catiomer.

Results and Discussion

Ordered fragmentation of pDNA by S1 nuclease was found when pDNA was complexed with PEG-PLys (PEG 12 kDa, PLys 17 units) prepared at a stoichiometric charge ratio [molar ratio between amine cations (N) in PLys and phosphate anions (P) in nucleotides (N/P ratio) = 1], as shown in Figure 1a. We have previously reported this ordered fragmentation behavior for three different pDNAs,[25] pBR322 (4361 bp), pGL3-Luc (5256 bp), and ColE1 (6641 bp), suggesting that S1 nuclease-specific fragmentation may commonly occur regardless of pDNA size. Here, S1 nuclease activity was extensively examined for a set of pDNAs ranging from 2 kbp to 12kbp. As shown in Figure 1b, ordered fragmentation by S1 nuclease was clearly observed for all pDNAs examined. It is obvious that the fragmentation pattern shifted upstream toward a higher molecular weight with increasing pDNA size, suggesting that S1 nuclease cleavage may occur at specific ratios proportional to the original pDNA size. Fragment lengths were estimated from the gel electrophoresis pattern and are shown as ratios with respect to the original pDNA length in Table 1. Interestingly, the fragment ratios were the same regardless of the pDNA size, with fragment lengths summarized as x/12. These results indicate that conservation of the ordered fragmentation is a phenomenon inherent to the condensed pDNA structure itself with unique geometrical characteristics.

(21) Katayose, S.; Kataoka, K. *Bioconjugate Chem.* **1997**, *8*, 702–707.
(22) Vinogradov, S.; Batrakova, E.; Li, S.; Kabanov, A. *Bioconjugate Chem.* **1999**, *10*, 851.
(23) Itaka, K.; Yamauchi, K.; Harada, A.; Nakamura, K.; Kawaguchi, H.; Kataoka, K. *Biomaterials* **2003**, *24*, 4495–4506.
(24) DeRouchey, J.; Walker, G. F.; Wagner, E.; Radler, J. O. *J. Phys. Chem. B* **2006**, *110*, 4548.
(25) Osada, K.; Yamasaki, Y.; Katayose, S.; Kataoka, K. *Angew. Chem., Int. Ed.* **2005**, *44*, 3544–3548.

Table 1. Fragment Lengths and Ratios with Respect to the Original pDNA Length for Various pDNAs Complexed by PEG-PLys Block Catiomer

	fragment length (bp)/size ratio with respect to the original pDNA (%)										
no.	pKF18 (2204 bp)	pUC19 (2686 bp)	T7 (4315 bp)	pBR322 (4363 bp)	pGL3-Luc (5256 bp)	ϕX174 (5386 bp)	Col E1 (6646 bp)	pAUR224 (7638 bp)	pPTR2 (10032 bp)	pAUR316 (11613 bp)	ratio as a fraction
1				3638/83.4	4545/86.5		5526/83.1				10/12
2	1635/74.2	1934/72.0	3311/76.7	3358/77.0	4003/76.2	4115/76.4	4966/74.7	5747/75.2			9/12
3	1429/64.8	1760/65.5	1760/67.0	2991/68.6	3631/69.1	3637/67.5	4468/67.2	4890/64.0	6000/59.8		8/12
4	1076/48.8	1297/48.3	2023/46.9	2227/51.0	2728/51.9	2551/47.4	3384/50.9	3700/48.4	4567/45.5	5375/46.3	6/12
5	724/32.8	888/33.1	1357/31.4	1469/33.7	1832/34.9	1773/32.9	2227/33.5	2435/31.9	3200/31.9	3732/32.1	4/12
6	534/24.2	669/24.9	1036/24.0	1083/24.8	1372/26.1	1301/24.2	1673/25.2	1870/24.5	2450/24.4	2824/24.3	3/12
7	359/16.3	719/16.8	710/16.5	728/16.7	911/17.3	894/16.6	1093/16.4	1232/16.1	1702/17.0	1871/16.1	2/12

S1 nuclease cleavage sites were identified by sequencing the cleaved fragments, extracted from electrophoresed gels; their sequences examined from both ends (see Supporting Information, Figure S1a). Sequencing analysis showed that cleavage sites were distributed in a nonspecific manner for all examined fragments (Figure S1b). Ultimately, no characteristic sequences related to DNA secondary structures[5] were found in the fragments such as A-T-rich or G-C-rich regions known to be Z-form preferred sequences, large palindrome sequences which are known to convert to cruciform extrusions, or purine-pyrimidine mirror repeats which facilitate intermolecular triplex formation. Note that the fragment lengths obtained from the determined cleavage sites by sequencing analysis corroborated well with those obtained from gel electrophoresis analysis (Supporting Information, Table S1).

Since the cleavage of pDNA by S1 nuclease occurred without any clear correlation to particular sequences characteristic of secondary structures, it is therefore assumed that double-strand breakage to expose the S1 nuclease-susceptible single strand may involve a more general scheme directly related to the folding process of the rigid pDNA molecule itself. It is plausible that double-stranded DNA may dissociate into single strands at the folding sites because double-stranded DNA is considerably rigid, with a persistent length (l_p) of approximately 50 nm,[15] and is not easily folded. However, single-stranded DNA is more flexible and easier to fold, with an l_p of only a few nanometers[26] or less.[27]

Folded structures of pDNA were investigated by AFM to examine the correlation between DNA folding and S1 nuclease activity. AFM images showed that pDNA is condensed into rod and toroid structures (Figure 1c). In rod structures, DNA must be folded in hairpin turns at rod ends, which may be responsible for the S1 nuclease activity. Therefore, rod lengths were measured to confirm any correlation between DNA folding and S1 nuclease activity. The measurement was performed by TEM with uranyl acetate (UA) staining to obtain an accurate length for the rod structures. It should be noted that UA associates with DNA more strongly than with PEG, so DNA is selectively observed in the TEM images. Interestingly, rod length distributions occurred in a specific manner, as shown in Figure 1d. The discrete distributions suggest a highly regulated process of pDNA condensation into rod structures with characteristic lengths. The rod length distributions are centered at approximately 610, 305, 190, 150, 115, 100, and 75 nm, and normalization of these lengths with respect to the 610 nm rod results in length ratios of 1, 1/2, 1/3, 1/4, 1/5, 1/6, and 1/8, respectively.

To further understand of the standard rod length of 610 nm, the theoretical rod length was estimated from the pDNA length. The contour length of pBR322 (4361 bp) is calculated to be 1474 nm using 0.338 nm/bp (as determined by X-ray crystallography) for B-form DNA. Therefore, a rod structure formed by simply collapsing the circular DNA along the diameter would be half the contour length (737 nm). The resulting rod structure would be in a twisted coiled-coil form due to the inherent superhelicity of pDNA, illustrated as structure (i) in Figure 2a, which would somewhat shorten the rod length. Using the superhelix density value of $\rho = -0.039$ known for native pDNA[28] and a linking number of 415.3 [obtained from 4361 bp/10.5 bp (helical pitch)], pBR322 intertwines 16 times (0.039×415.3) along the long axis. The length of the twisted rod structure is calculated to be 730 nm (the estimation procedure is described in detail in the Supporting Information). Furthermore, the observed DNA contour length in TEM images obtained with UA staining and a collodion substrate is 83.7%[29] of the calculated DNA length, based on 0.338 nm/bp. Thus, the rod length (structure (i) in Figure 2a) is calculated to be 611 nm ($= 0.837 \times 730$ nm), which coincides nicely with the longest rod length observed empirically (Figure 1d).

From the characteristic patterns of cleavage by S1 nuclease and rod size distributions observed in condensed pDNA, we propose a quantized folding model to explain the highly regulated pDNA condensation process (illustrated in Figure 2a). In this proposed model, the lengths of the rod structure folded once (structure (ii) in Figure 2a), twice (structure (iii)), and three times (structure (iv)) are determined to be 306, 204, and 153 nm, respectively, using the theoretically estimated rod length of 611 nm for the initial rod structure (structure (i)). The estimated rod lengths, which are indicated by dotted lines in

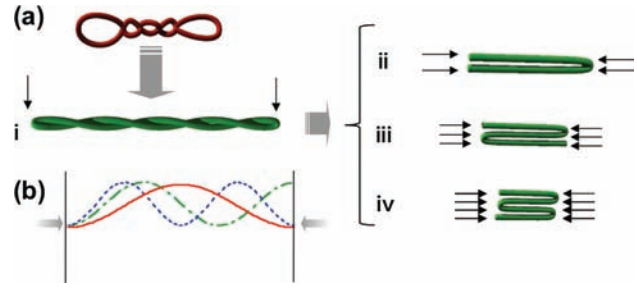

Figure 2. Mechanism of pDNA condensation into rod structures with regulated folding. (a) Formation of rod structures in a quantized manner: (i) unfolded rod structure, (ii) rod structure with a single fold, (iii) rod structure with two folds, and (iv) rod structure with three folds. S1 nuclease-susceptible sites (sites of single-stranded DNA induced by the dissociation of double-helical DNA) are indicated by arrows. For simplification, intertwining due to the superhelicity is not pictured in the folded rods (ii−iv). (b) Deformation modes of rod structures predicted by the Euler buckling theory.

(26) Tinland, B.; Pluen, A.; Sturm, J.; Weill, G. *Macromolecules* **1997**, *30*, 5763–5765.
(27) Smith, S. B.; Cui, Y. J.; Bustamante, C. *Science* **1996**, *271*, 795–799.

Table 2. Expected Fragment Ratios and Lengths of the Rod Structures in the Quantized Folding Model

	expected fragment ratios from the quantized folding model[a]						shown
	$n = 0$	$n = 1$	$n = 2$	$n = 3$	$n = 4$	$n = 5$	as $x/12$
	2/2	4/4	6/6	8/8	10/10	12/12	12/12
						11/12	
					9/10		
				7/8			
			5/6			10/12	10/12
					8/10		
		3/4		6/8		9/12	9/12
					7/10		
			4/6			8/12	8/12
				5/8			
					6/10		
						7/12	
	1/2	2/4	3/6	4/8	5/10	6/12	6/12
						5/12	
					4/10		
				3/8			
			2/6			4/12	4/12
					3/10		
		1/4		2/8		3/12	3/12
					2/10		
			1/6			2/12	2/12
				1/8			
					1/10		
						1/12	
multiples	$x/2$	$x/4$	$x/6$	$x/8$	$x/10$	$x/12$	
expected length[b]	611 nm	306 nm	204 nm	153 nm	122 nm	102 nm	

[a] Ratio with respect to the original pDNA length. n indicates the number of folds. [b] Estimated rod length from the TEM images considering shrinkage due to the supercoiling and UA staining on the collodion substrate.

Figure 1d, are in good agreement with the rod lengths measured from the TEM images, thus strongly supporting the quantized folding model proposed here.

Dissociation of double-stranded DNA must occur at the rod ends to allow folding as proposed in this model. There are two possible folding sites for formation of the initial rod structures (structure (i) in Figure 2a), as indicated by arrows. Cleavage by S1 nuclease at only one site results in the linearization of the parent pDNA, and cleavage at both sites results in a pair of half-length fragments of the parent pDNA. Consequently, the expected fragment lengths produced from the initial rod structure are multiples of 1/2 (1/2 and 2/2). In the same manner, expected fragments from the rod structure folded once (structure (ii)) are multiples of 1/4 because there are two double-strand dissociation sites at one end. Furthermore, the expected fragment fractions are multiples of 1/6 and 1/8 for rods folded twice (structure (iii)) and three times (structure (iv)), respectively. The expected fragment fractions from the proposed model are summarized as multiples of $1/2(n+1)$ for rods folded n times, as listed in Table 2. Ultimately, fragments of length corresponding to fractions of $x/12$ frequently appear; in particular, the fractions of 12/12 and 6/12 appear most frequently. Note that the bands corresponding to 12/12 (linear) and 6/12 (band 4) are observed as the two strongest intensities in the gel electrophoresis profiles (Figure 1a).

To obtain further insight into S1 nuclease digestion activity at the rod ends of the folded pDNA, AFM imaging was conducted in the presence of S1 nuclease under aqueous

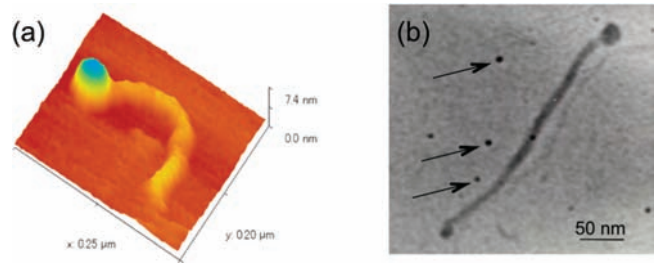

Figure 3. AFM (a) and TEM (b) images of pDNA (pBR322) rod structure in the presence of S1 nuclease. Note the spherical structures observed at the rod ends. Arrows in the TEM image (b) indicate free S1 nucleases, seen as 8 nm particles.

conditions. Rods with a sphere structure at the rod ends were observed, as shown in Figure 3a. The sphere size was estimated to be approximately 40 nm from the AFM images, which is rather large assuming this sphere structure to be a single S1 nuclease. Presumably, more than one S1 nuclease is involved in the observed sphere, as there are multiple S1 nuclease recognition sites (single strands) at the rod ends. TEM observation in the presence of S1 nuclease also gave similar images (Figure 3b). Considering that S1 nucleases were observed as 8 nm particles in the TEM images, as indicated by the arrows in Figure 3b, it is reasonable to assume that the observed sphere structure may be an S1 nuclease cluster. These direct observations by AFM and TEM provide strong evidence of S1 nuclease binding to the rod ends where acute DNA folding occurs with double-strand dissociation.

In the quantized folding model, the unfolded rod structure (structure (i) in Figure 2a) is considered as an initial condensed structure. This structure may be favorable in the early stages of the condensation process because S1 nuclease activity toward complexed pDNA prepared at an N/P ratio of 0.75 showed only two major bands, corresponding to 1 (linear) and 1/2 of the parent pDNA length (Figure 1e), suggesting that structure (i) in Figure 2a is the dominant form under these conditions. The unfolded structure (i) may be energetically favorable because it is formed by minimal conformational changes of naked pDNA and requires the lowest bend energy (only at both rod ends), leading to double-strand dissociation to release the bending stress through the formation of more-flexible single strands.

The increased rigidity of the initial rod structures resulting from intertwining coiled-coil formation and geometrical folding with sequence independence led to the hypothesis that folding may occur so as to release mechanical stress present in the rod structure. In this regard, Euler buckling, a well-known theory explaining the mechanical deformation of a rod structure in structural dynamics, may be applied here. According to this theory, a rod of length l fluctuates in a regular fashion, buckling at $l/2$, $l/3$, $l/4$, ..., taking free and roller ends as boundary conditions, as shown in Figure 2b. If the unfolded rod structure (i) fluctuates according to the Euler buckling theory, rods can be folded at each vertex and quantized (Figure 2).

In order to adopt the Euler buckling theory into the quantized folding model of pDNA condensation, it is necessary to place compression force on the rod. Condensation of pDNA is principally caused by charge neutralization upon polyion complexation with cationic compounds. Negatively charged pDNA is hydrated in solution with a spatially expanded conformation due to positive osmotic pressure originating from electrostatic repulsion, entropic elasticity, solvation of the DNA chain, counterions, and mixing entropy. Upon complexation,

(28) Gray, H. B.; Upholt, W. B.; Vinograd, J. *J. Mol. Biol.* **1971**, *62*, 1–19.
(29) Namork, E.; Johansen, B. V. *Micron* **1980**, *11*, 85–90.

counterions are released into solution, leading to an increase in translational entropy, and the dehydrated DNA chain accommodates negative osmotic pressure, resulting in condensation into a compact form to decrease surface free energy. Attraction force developing along the DNA chain may be integrated toward the center of the rod structure (i) in Figure 2a to induce rod compression.

To verify the applicability of the Euler buckling theory to pDNA folding by PEG-PLys block catiomer binding, the rigidity of the initial rod structure (structure (i) in Figure 2a) was estimated for the complex of pUC19 (details in Supporting Information). Briefly, the unfolded rod structure was selectively prepared by titration mixing of pDNA with PEG-PLys block catiomer. The hydrodynamic radius (R_h) of the complex was then obtained on the basis of dynamic light scattering (DLS) measurement from the Einstein−Stokes equation using the overall translational diffusion constant (D_0), which includes structural anisotropy. Given the worm-like chain model,[30] the l_p obtained from R_h was calculated to be 88.7 nm, leading to a bending modulus of $\kappa = 3.65 \times 10^{-28}$ N·m^2, as determined from $\kappa = l_p k_B T$. Note that κ for double-stranded DNA is reported[31] to be 2×10^{-28} N·m^2; thus, the value determined for the rigidity of the initial rod structure seems to be reasonable, considering the increased rigidity resulting from formation of the intertwining coiled-coil structure. Finally, the bending elastic modulus (E) was obtained from the equation $\kappa = EI$ (where I is the second moment of area) to be 0.12 GPa, which is of the same order of magnitude as that of microtubules[32] and 1 order of magnitude smaller than that of f-actin,[33] both of which are known to exhibit buckling deformation. As for the correlation of l_p with Euler buckling fluctuations, there is a critical length (L^*) for Euler buckling, as expressed in the following equation:[34]

$$L^{*3} = 4\pi^4 R^2 l_p$$

Using $l_p = 88.7$ nm, L^* is calculated to be 133.5 nm, which is shorter than the rod length of the unfolded pUC19 (500 nm). This result indicates that the initial rod structure satisfies the conditions of mechanical buckling, supporting the applicability of the Euler buckling theory to the ordered folding of pDNA observed here.

According to the Euler buckling theory, increased folding requires a higher load to occur; thus, it is expected that the frequency of each folded structure may decrease with increased folding. The frequency of structures with different degrees of folding can be estimated from the rod length distribution data shown in Figure 1d (also shown in Figure S5 in the Supporting Information). The observed size distributions revealed that the once-folded structure occurred most frequently, and the frequency decreased with increasing folding number n. This trend is consistent with the gel electrophoresis data in Figure 1a, and these results support the Euler buckling model proposed in this study. Note that the fragments of rods folded more than three times, i.e., $x/8$, $x/10$, $x/12$, ..., were not clearly seen in Figure 1a, although they are expected from the model as indicated in Table 2, and are predicted from the Euler buckling theory.

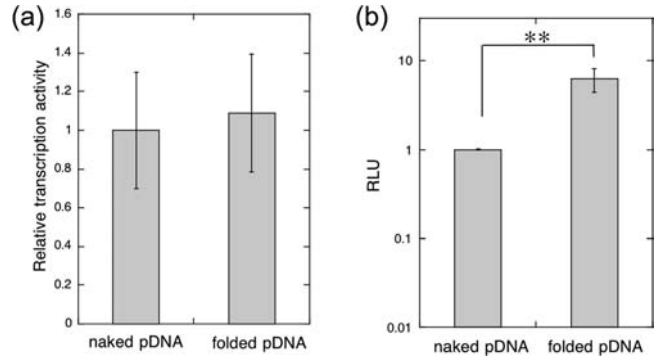

Figure 4. *In vitro* transcription efficiency (a) and gene expression efficiency (b) of complexed and naked pDNA. (a) Transcription efficiency was evaluated in a solution containing elements necessary for transcription. The amount of transcribed RNA was normalized to that of naked pDNA ($n = 4$, mean ± SD). (b) Gene expression efficiency was evaluated in a cell-free system. Relative light units (RLU) of luciferase expression were normalized to naked pDNA ($n = 6$, mean ± SD).

Presumably, folding with higher numbers occurs less frequently as described above, and eventually the intensity of these fragments may be lower than the detection limit. Indeed, the fragments expected from rods formed with three, four, and five folds were observed by using the block catiomers with different PLys chain lengths; details will be reported elsewhere in the near future. The good agreement between theory and observation justifies the application of the Euler buckling theory to the quantized DNA folding observed here, which is consistent with the theoretical prediction of DNA condensation by Manning based on the buckling scheme.[35]

It should be noted that toroid structures are observed in AFM and TEM along with rod structures. The exact relationship between toroid and rod structures has not been clarified, but several studies based on TEM and AFM imaging techniques showed that toroid structures are formed by the bending of rods followed by the fusion of their ends or by the rods opening.[16] Furthermore, rods and toroids frequently undergo mutual transition in a dynamic manner.[36−38] According to these observations, toroid structures may be structural isomers of the rod structures.

It is of interest to investigate the transcription/translation activity of pDNA regularly folded by PEG-PLys, particularly from the standpoint of developing novel gene carrier systems. Therefore, the transcription efficiency was examined in a solution containing transcription components, i.e., ribonucleotides and RNA polymerase. As shown in Figure 4a, the regularly folded pDNA showed transcription efficiency comparable to that of naked pDNA, indicating that the complexation of pDNA with PEG-PLys is not the limiting factor for transcription. It is worth noting that the relative gene expression efficiency was even higher for folded pDNA compared to naked pDNA in the cell-free transcription/translation assay system for luciferase expression (Figure 4b). The most plausible reason for this apparent increase in gene expression efficiency is the

(30) Hayakawa, H. *Annu. Rev. Phys. Chem.* **1974**, *25*, 179–200.
(31) Matsumoto, A.; Go, N. *J. Chem. Phys.* **1999**, *110*, 11070–11075.
(32) Kis, A.; Kasas, S.; Babic, B.; Kulik, A. J.; Benoit, W.; Briggs, G. A. D.; Schonenberger, C.; Catsicas, S.; Forro, L. *Phys. Rev. Lett.* **2002**, *89*, 248101.
(33) Ishijima, A.; Harada, Y.; Kojima, H.; Funatsu, T.; Higuchi, H.; Yanagida, T. *Biochem. Biophys. Res. Commun.* **1994**, *199*, 1057–1063.
(34) Manning, G. S. *Phys. Rev. A* **1986**, *34*, 4467–4468.
(35) Manning, G. S. *Biopolymers* **2003**, *69*, 137–143.
(36) Dunlap, D. D.; Maggi, A.; Soria, M. R.; Monaco, L. *Nucleic Acids Res.* **1997**, *25*, 3095–3101.
(37) Martin, A. L.; Davies, M. C.; Rackstraw, B. J.; Roberts, C. J.; Stolnik, S.; Tendler, S. J. B.; Williams, P. M. *FEBS Lett.* **2000**, *480*, 106–112.
(38) Rackstraw, B. J.; Martin, A. L.; Stolnik, S.; Roberts, C. J.; Garnett, M. C.; Davies, M. C.; Tendler, S. J. B. *Langmuir* **2001**, *17*, 3185–3193.

increased tolerability of the folded pDNA against nuclease attack.[39] The cell-free transcription/translation assay solution was reconstructed from cell lysate and thus contains a finite amount of nuclease. Indeed, an appreciable tolerability against DNase I was confirmed for the folded pDNA, while the naked pDNA was promptly digested under the same conditions (see Supporting Information). This result, in turn, suggests that the PEG-PLys complex with pDNA has significant stability in the biological milieu; thus, spontaneous dissociation of the PEG-PLys/pDNA complex is unlikely to occur, which would allow for efficient transcription. Apparently, this finding is inconsistent with the comparable transcription efficiency of the folded pDNA with the naked pDNA, as shown in Figure 4a, because the tight binding of PEG-PLys to pDNA should impede transcription by RNA polymerase. Presumably, selective exchange of PEG-PLys with transcription factors and RNA polymerase may occur on the DNA strands in the process of transcription; however, further detailed research is needed to verify this assumption.

In a practical sense, the enhanced gene expression of pDNA folded by PEG-PLys in the biological milieu, as seen in Figure 4b, is appealing for the design of gene carrier systems with therapeutic potential. Indeed, we have recently demonstrated the utility of the PEG-PLys/pDNA system for *in vivo* gene transfer of the soluble form of vascular endothelial growth factor receptor (sFlt-1) to skeletal muscle, thereby succeeding in inhibiting tumor growth through an anti-angiogenic effect.[40]

Conclusion

In this study, we have demonstrated the highly regulated folding of pDNA upon complexation with PEG-PLys block catiomer to form rod structures with characteristic lengths. This observed phenomenon is consistent with the proposed quantized folding model, which may be explained by mechanical buckling of coiled-coil rods. Extension of this finding may provide a reasonable model to elucidate the packaging mechanism of supercoiling DNA structures in nature, such as the packaging of mitochondria and the bacterial genomes (which both have a supercoiled closed-circular form in their nucleoids) and also chromatin architectures of different hierarchy stages, each exhibiting superhelicity. Furthermore, the packaging of pDNA with regular folding into a polyion complex core surrounded by a PEG palisade was shown to be a promising strategy for constructing nonviral gene carrier systems that may be useful even in harsh biological environments.

Acknowledgment. This work was financially supported by the Core Research Program for Evolutional Science and Technology (CREST) from the Japan Science and Technology Corporation (JST), the Center for Medical System Innovation (CMSI, Global COE Program, MEXT), and the Tokyo Ohka Foundation for the Promotion of Science and Technology. The authors also appreciate Dr. R. James Christie for grammatical correction of the manuscript.

Supporting Information Available: Sequencing analysis of the S1 nuclease cleaved fragments, contribution of superhelicity to rod length, length determination of pDNA rods condensed by PEG-PLys block catiomer, estimation of rigidity in the unfolded coiled-coil rod structure, frequency of folding number, tolerability against nuclease, and Materials and Methods. This material is available free of charge via the Internet at http://pubs.acs.org.

JA102739B

(39) Katayose, S.; Kataoka, K. *J. Pharm. Sci.* **1998**, *87*, 160–163.
(40) Itaka, K.; Osada, K.; Morii, K.; Kim, P.; Yun, S.-H.; Kataoka, K. *J. Controlled Release* **2010**, *143*, 112–119.